CHEMICAL ENGINEERING TRANSACTIONS
VOL. 43, 2015
A publication of AIDIC
The Italian Association of Chemical Engineering
Online at www.aidic.it/cet
Chief Editors: Sauro Pierucci, Jiří J. Klemeš

ISBN 978-88-95608-34-1; **ISSN** 2283-9216
DOI: 10.3303/CET1543274

3D Simulation and Validation of a Lab Scale Bubble Column

Thomas Eppinger*[a], Matheus Herckert [a], Ravindra Aglave[b]

[a]CD-adapco, Nordostpark 3-5, 90411 Nürnberg, Germany
[b]CD-adapco, 11000 Richmond Ave., Suite 100Houston, TX
thomas.eppinger@cd-adapco.com

Bubble columns are widely used in the chemical, petrochemical and biochemical industry. The correct prediction of the fluid dynamics, gas hold-up and bubble size distribution is of importance for the design and development of such reactors. For this, experimental as well as numerical methods are widely used to study these reactors, since the numerical simulations have made significant progress in the last years for this kind of multiphase flow.
In this contribution we have investigated numerically 3D lab scale bubble columns to validate the predictive capabilities of the commercial CFD solver STAR-CCM+ by CD-adapco. For the simulation of the two phase flow an Eulerian-Eulerian approach was used. Several forces which interact between both phases are taken into account: drag force, lift force, turbulent dispersion force, virtual mass force and the turbulence induced by bubbles.
Validation is done with respect to plume oscillation frequency, liquid and bubble velocity and gas holdup against published data. A reasonable agreement between the numerical and experimental results was found. Further the importance of the different interaction forces could be shown: the virtual mass force is of minor importance, while the lift force influences strongly the oscillation of the plume.

1. Introduction

Bubble columns are easy to construct and have low operating costs. They are used in a variety of chemical processes such as hydrogenation, catalytic slurry reactors and gas absorption for natural gas treatment with amines etc. Bubble columns are essentially liquid filled vessels in which gas bubbles through single or multipoint devices called spargers. Spargers can be perforated plates or rings. The diameters of the holes used in the spargers, viscosity and surface tension of the liquid, height to diameter ratio of the column, presence of internal baffles are some of the parameters that define the final gas hold up characteristics. Gas hold up is a key characteristic of the bubble columns which governs the interfacial area and in turn the overall performance.
The flow behaviour of bubble columns has been of interest for several decades and many researchers have investigated the columns experimentally in terms of gas holdup and liquid circulation (Freedman and Davidson (1969)), on the effect of sparger design and gas holdup (Thorat et al. (1998)) and on the flow pattern and plume oscillation (Becker et al. (1994)) as well as numerically, where Pfleger et al. (1999) developed a model to reproduce the experimental results by Becker et al. (1994), Diaz et al. (2008) extended the model to include bubble size distribution and non-drag forces, while Ziegenhein et al. (2013) showed the influence of polydispersity and higher gas flow rates on a large scale column with a height of 2.5m and Silva Jr. et al. (2013) studied the hydrodynamics inside a slurry bubble column.
Experimental investigations involved studying the effect of the above mentioned parameter for one or more gas-liquid pair or system. The results can typically be correlated using dimensionless number or other parameters. However, each new design and system often needs repeat of experimental work for a new plant and its scale-up. Numerical methods therefore have been adopted which can ease this work because simulation can allow to investigate large number of parameters for virtually any gas-liquid pair.
Flow of the gas through the liquid can give rise to swarms of bubble that are similar in size (homogeneous regime) or distinctly varying (churn turbulent or heterogeneous regime). There is significant amount of

Please cite this article as: Eppinger T., Matheus H., Aglave R., 2015, 3d simulation and validation of a lab scale bubble column, Chemical Engineering Transactions, 43, 1639-1644 DOI: 10.3303/CET1543274

coalescence or break-up of bubble that occurs in the heterogeneous regime. The simulation presented in this work uses a general purpose code (finite volume code STAR-CCM+ v8.04 by CD-adapco) with the Eulerian framework. Mass and momentum conservation equation for each of the phases in the domain are solved.

Figure 1: Geometry of the investigated bubble column. The sensor point in the centre (h = 0.225 m, w = 0.1 m, d = 0.025 m) is used to determine the oscillation frequency and amplitude.

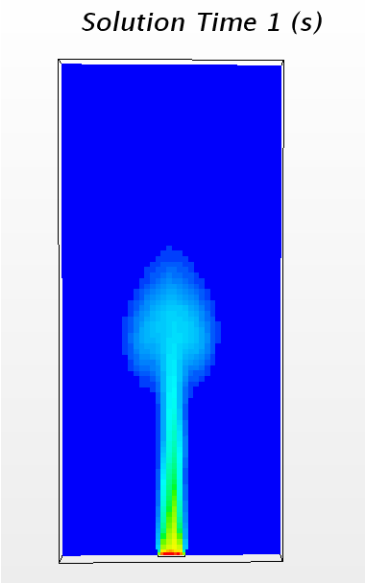

Figure 2: Air distribution after 1s shows the well-known mushroom-shaped plume, see e.g. Pfleger et al.(1999).

There is one continuous phases and one or more dispersed phases that can be described in the framework. Eulerian framework allows the treatment of the numerous bubbles as a single phase which reduces the computational time compared to an explicit treatment of the bubbles significantly. Multiple sizes can be treated as separate phases as well. The interaction between the phases is described using various interaction force parameters. The movement of bubbles relative to the liquid is governed by these interaction forces acting on the bubbles, which are explained in the later sections. Calculating these forces is necessary to accurately capture the bubble behaviour.

2. Methodology – Base Case

The referenced experimental setup is described in detail in Becker et al. (1994). It is basically a rectangular column with a width of w = 0.2 m, a depth of d = 0.05 m and a height of h = 0.45 m, which is equal to the fill level of tap water. In the centre at the bottom a gas sparger plate distributes the air bubbles. A schematic sketch is shown in Figure 1.

The base case setup follows the description given by Pfleger et al. (1999). Based on the results of the base case simulations several changes were made, which are described and discussed in section 3.

For the base case the geometry is meshed with approx. 40,000 hexahedron cells with a constant edge length of 5mm. A velocity inlet is used as boundary condition for the sparger inlet, where only air enters the domain ($\dot{V}_{gas} = 48\ l/h$) with the terminal rise velocity of a single bubble (v = 0.2 m/s). The total mass or volume flow is adjusted via the volume fraction. At the top a degassing boundary condition is used which is fully permeable for gas (zero gradient), but impermeable for water (slip wall condition). All other boundaries are no-slip wall conditions. The continuous incompressible fluid with constant properties is tap water (dynamic viscosity $\eta = 8.89 \cdot 10^{-4}$ Pa·s; density $\rho = 997.5$ kg/m³). For the disperse air phase ($\eta = 1.86 \cdot 10^{-5}$ Pa·s; $\rho = 1.18$ kg/m³) a constant bubble diameter of dp = 2 mm is assumed, because of the relatively low gas flow rate, which leads to a homogeneous flow regime. Turbulence is modelled with the realizable k-ε model and to capture the flow behaviour like the oscillation of the gas plume, all simulations are run in transient with a time step size of dt = 0.01 s.

The two-phase flow is modelled with an Eulerian multiphase model, where for both phases, the continuous water phase and the disperse gas phase, two complete sets of Navier-Stokes equations are solved. These equations are coupled by the volume fraction and the forces which are interacting between both phases. For

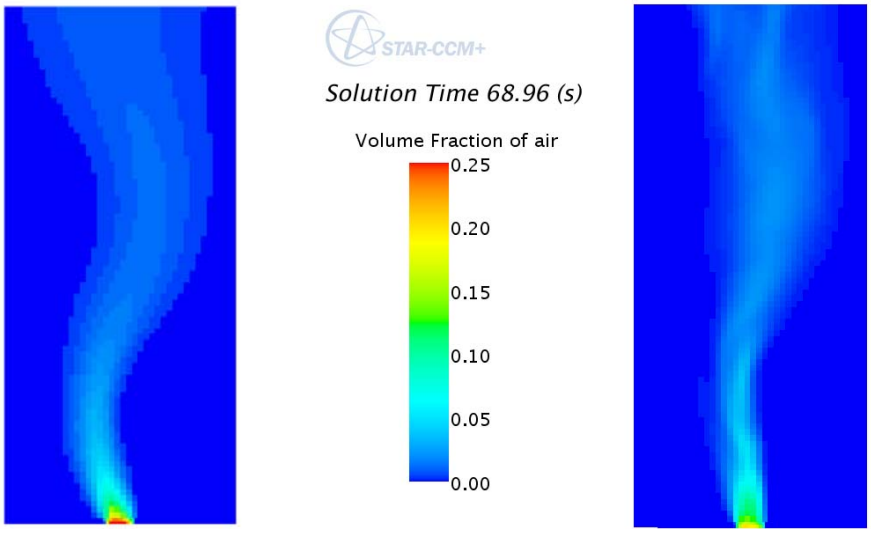

Figure 3: Left: Gas bubble plume for the base case. The shape is relatively well defined and oscillation period and amplitude are regular. Right: Gas bubble plume for the enhanced case, where further forces like the lift force are considered. The plume shape spreads and its oscillation shows more stochastic fluctuations.

the base case, only buoyancy, drag force with a constant drag force coefficient of Cd = 0.66 and turbulent dispersion force are considered.

2.1 Results – Base Case

The simulation results are compared with experimental data from Becker et al. (1994) as well as with numerical results by Pfleger et al. (1999) with respect to plume oscillation frequency and amplitude and gas holdup.
Gas starts to enter the reactor with quiescent water at the sparger at the bottom. Due to the upward directed force the gas bubbles start to rise. After a simulation time of 1s the typical mushroom shaped bubble plume is found like depicted in Figure 2. After the bubbles break through the surface at the top, the plume stays almost quite in the centre of the column for some seconds. Temporal instabilities in vortices to the right and left of the plume due to the acceleration of the continuous water phase leads to a sideward movement of the plume, which influences the vortices in the continuous phase and which results finally in the well-known oscillation of the plume as shown in Figure 3 on the left.
The vortices in the liquid phase at a given time are visualized in Figure 4. It can be clearly seen how these

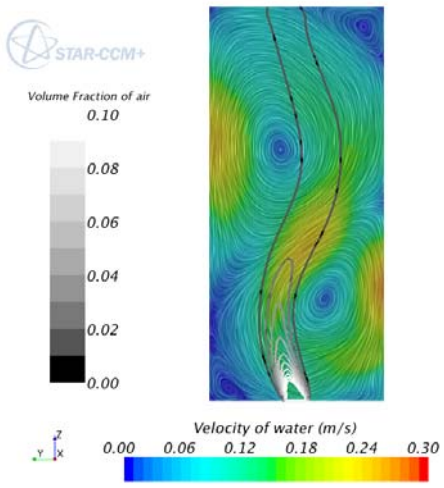

Figure 4: Instantaneous liquid velocity field. Liquid vortices are influencing the gas bubble path significantly.

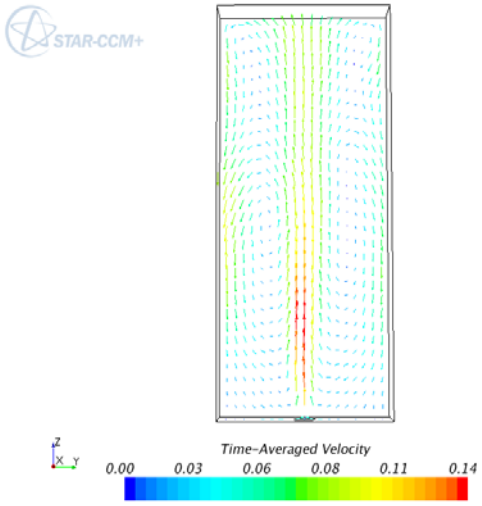

Figure 5: Liquid velocity, averaged over 100s.

vortices influence the path of the bubbles due to the drag force. These vortices are temporary vortices which are moving through the reactor. This can be seen in Figure 5, where the liquid velocity field averaged over 100 s is shown: On average, the gas bubbles are rising in the centre of the reactor and due to the drag force, water is accelerated upwards. Due to continuity reasons the water phase must flow down in the vicinity of the walls and in average a constant circulating liquid velocity field is observed.
In the centre point of the reactor (see Figure 1) the horizontal water velocity over time is tracked and the resulting plot is given in Figure 6. A very regular oscillation of the plume starts shortly after bubbles are reaching the top surface. The amplitude of the oscillation is increasing and reaches its maximum of approximately ±0.2 m/s after 5 to 6 full oscillations. A period lies in a range of 15 s. Similar numerical results are reported by Pfleger et al. (1999): the horizontal liquid velocity range is slightly above ±0.2 m/s and the oscillation period is reported with 15-20 s.
Although the simulation results are in quite good agreement with the numerical results by Pfleger et al.(1999) the discrepancy to experimental data with respect to plume oscillation amplitude and the form of the oscillation is still high. At this point the inclusion and influence of other phase interaction forces has to be discussed.

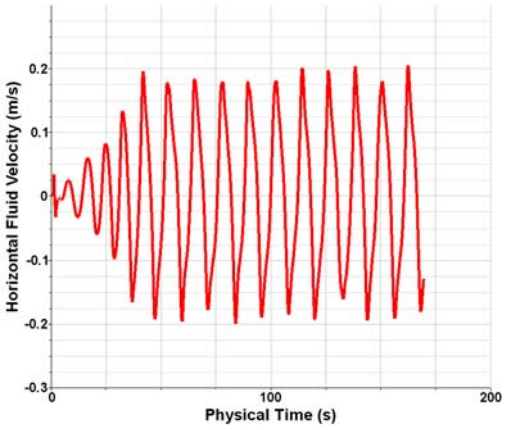

Figure 6: Plume oscillation period and amplitude for the base case.

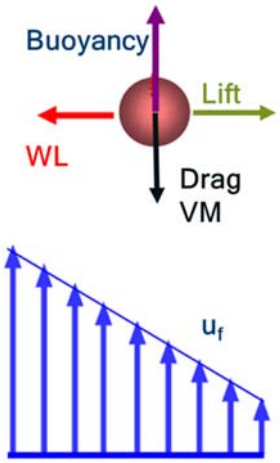

Figure 7 Forces acting on a bubble travelling through a liquid velocity field u_f. WL stands for wall lubrication and VM for virtual mass.

3. Enhanced Model

In the past 15 y several computational studies have been performed on the dynamics of bubble plumes.
Since the conclusions of the different authors are partly contradictory we included in our study several phase interaction forces to judge their influence on the results. The drag force is changed to the drag force model by Tomiyama et al. (1998), which is applicable for a wide range of Eötvös-, Reynolds- and Morton-number and covers more or less the whole range of possible bubble shapes. The lift force, which acts on bubbles travelling through a shear field, is included also based on the model given by Tomiyama et al. (2002). The Virtual Mass force takes the inertia from the surrounding fluid added to an accelerating bubble into account. Finally, bubble induced turbulence is included by the model of Troshko and Hassan (2001). Wall lubrication force, which only acts near to walls (within approximately 5 bubbles diameter from the wall), is omitted, since bubbles are not detected in the near wall region. These forces are shown schematically in Figure 7.
Domain, boundary conditions and numerical settings are the same as for the base case.

3.1 Results

A qualitative analysis shows, that the averaged liquid velocity as well as the liquid vortices are quite similar to the one of the base case (not shown). However, the shape of the oscillating plume is different. While for the base case shown in Figure 3, left, the shape is relatively compact and confined, the gas plume now spreads over a larger area or volume and the gas bubbles are distributed more randomly as shown in Figure 3 on the right. This is attributed to the additional forces which are now considered. The effect of these forces is shown

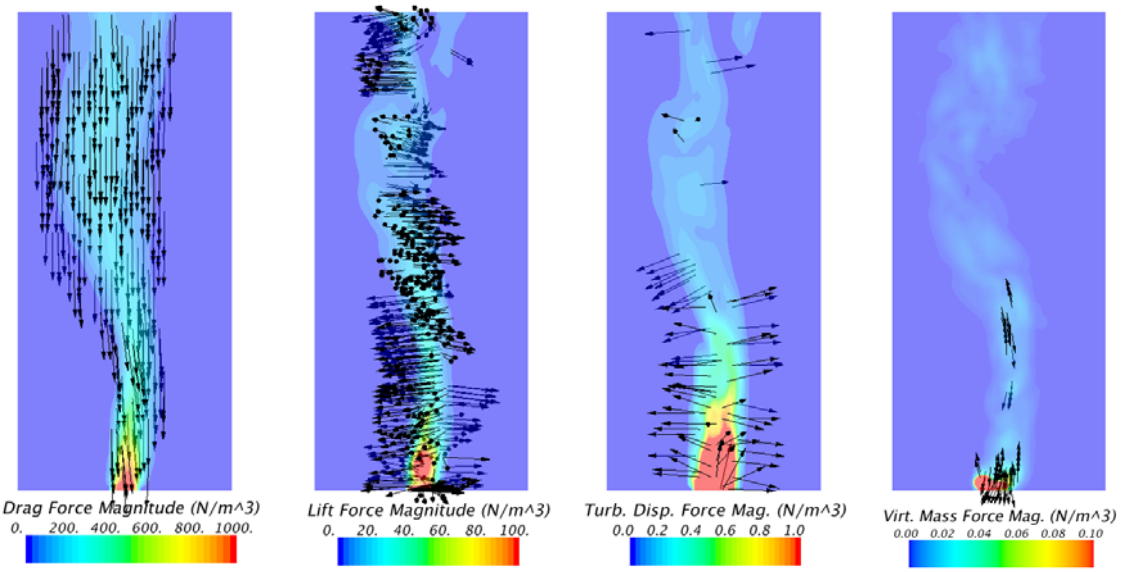

Figure 8: Absolute value und direction of different forces acting on the bubbles. From left to right: drag, lift, turbulent dispersion and virtual mass force. The absolute value of the forces is orders of magnitude different.

in Figure 8. The scalar value shows the magnitude of the forces, while the arrows show the direction in which they act. For a better visibility all vectors below 5 % of the maximum value are clipped and only a portion of the remaining vectors are shown. Note that the vectors are not scaled.

The most influencing force based on the absolute value is the drag force, followed by the lift force. The turbulent dispersion force as well as the virtual mass force is mostly acting directly above the sparger. The absolute value of the latter forces is relatively small, especially the virtual mass force: its maximum value is approximately 5 orders of magnitude smaller than the drag force.

While the drag and the virtual mass force are mainly acting in vertical direction, the lift and turbulent dispersion force are acting in horizontal direction and are responsible for the horizontal gas distribution as well as the plume shape and plume oscillation period. Especially the lift force contributes significantly (2 orders of magnitude larger than the turbulent dispersion force) and causes the different plume shape compared to the base case. These additional forces have also a significant influence on the plume oscillation and the amplitude as shown in Figure 9. The plume oscillation period is still in the range of 15-20 s, but now the oscillation itself is no longer as regular as in the base case: Random fluctuations of the bubble plume occur and the oscillation amplitude is reduced to a value of ±0.1-0.15 m/s. It is obvious that with a RANS turbulence model the turbulent fluctuations (the peaks in the experimental results) cannot be captured, but beside this the agreement between the experimental and numerical results is quite accurate.

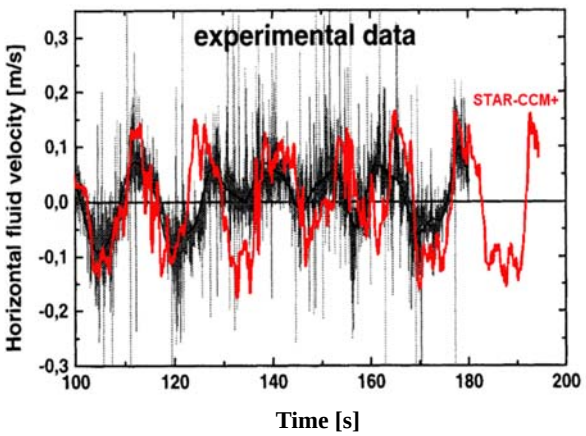

Figure 9: Comparison of the plume oscillation with experimental data from Becker et al.(1998).

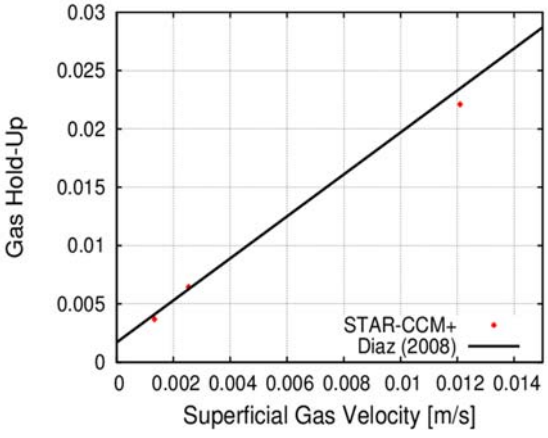

Figure 10: Comparison of the gas hold-up in the column for different gas flow rates with experimental data.

Finally in Figure 10 the gas holdup is compared with experimental results published by Diaz et al.(2008). In the simulation drag, turbulent dispersion and lift force are considered, but not the virtual mass force. Two additional volume flow rates ($\dot{V}_{gas2} = 92\ l/h$ and $\dot{V}_{gas3} = 450\ l/h$) were used to realize higher gas hold up. For all three investigated volumetric gas flow rate the predicted gas holdup agrees very well with the measurement data.

4. Conclusion

The aim of this work was to show the predictive capabilities of the finite volume CFD code STAR-CCM+ by CD-adapco with respect to bubble columns. The numerical results were compared with experimental result from literature for a 3D bubble column working in the homogeneous flow regime and show a quite good agreement in terms of gas plume oscillation frequency and amplitude. Also the gas hold-up, which is an important parameter for the design of bubble columns, is predicted accurately for different gas volume flow.
The importance of different forces, which are acting between the continuous liquid phase and the disperse gas phase, could be quantified: The virtual mass force and the wall lubrication force are of no importance in the investigated parameter range, but the turbulent dispersion force and especially the lift force are playing a significant role to predict the oscillation of the gas plume correctly.

Reference

Becker S., Sokolichin A., Eigenberger G., 1994, Gas-liquid flow in bubble columns and loop reactors: Part II. Comparison of detailed experiments and flow simulations. Chem. Eng. Sci., 49(24B), 5747-5762.

Dıaz M.E., Iranzo A., Cuadra D., Barbero R., Montes F.J., Galan M.A:, 2008, Numerical simulation of the gas–liquid flow in a laboratory scale bubble column Influence of bubble size distribution and non-drag forces, Chem. Eng. J., 139, 363-379

Freedman W., Davidson J. F., 1969, Hold-up and liquid circulation in bubble columns, Trans IChemE, 47, 251-262.

Pfleger D., Gomes S., Gilbert N., Wagner H.-G., 1999, Hydrodynamic simulations of laboratory scale bubble columns fundamental studies of the Eulerian-Eulerian modelling approach, Chem. Eng. Sci., 54, 5091-5099.

Silva Jr. J. L., Mori E. D., Soccol Jr. R., d'Avila M.A., Mori, M., 2013, Interphase Momentum Study in a Slurry Bubble Column, Chemical Engineering Transactions, 32, 1507-1512

STAR-CCM+ User guide, version 8.04, CD-adapco, Melville (NY), USA

Thorat B.N., Shevade A.V., Bhilegaonkar K. N., Aglave R. H., Parasu Veera U., Thakre S. S., Pandit A. B., Sawant S. B., Joshi J. B., 1998, Effect of sparger design and height to diameter ratio on fractional gas hold-up in bubble columns, Trans IChemE, 76, Part A, 823-834

Tomiyama A., Kataoka I., Zun I., Sakaguchi T., 1998, Drag Coefficients of single bubbles under normal and micro gravity conditions, JSME International Journal, Series B, 41(2), 472-479.

Tomiyama A., Tamai H., Zun I., Hosokawa S., 2002, Transverse migration of single bubbles in simple shear flows, Chem. Eng. Sci., 57, 1849–1858.

Troshko A. A., Hassan Y. A., 2001, A two-equation turbulence model of turbulent bubbly flows, International Journal of Multiphase Flow, 27, 1965-2000.

Ziegenhein T., Rzehak R., Krepper E. and Lucas D., 2013, Numerical Simulation of Polydispersed Flow in Bubble Columns with the Inhomogeneous Multi-Size-Group Model, Chemie Ingenieur Technik, 85,1080–1091.